

QCA, IVUS and OCT in interventional cardiology in 2011

Johan H.C. Reiber, Shengxian Tu, Joan C. Tuinenburg, Gerhard Koning, Johannes P. Janssen, Jouke Dijkstra

Division of Image Processing (LKEB), Department of Radiology, Leiden University Medical Center (LUMC), Leiden, The Netherlands

Corresponding to: Johan H.C. Reiber, PhD. Division of Image Processing (LKEB), Department of Radiology, Building 1C2-S, Leiden University Medical Center (LUMC), PO Box 9600, 2300 RC Leiden, The Netherlands. Tel:+31 71 526 3935. Email: J.H.C.Reiber@lumc.nl.

Abstract: Over the past 30 years, quantitative coronary arteriography (QCA) has been used extensively as an objective and reproducible tool in clinical research to assess changes in vessel dimensions as a result of interventions, but also as a tool to provide evidence to the interventionalist prior to and after an intervention and at follow-up when necessary. With the increasing complexities of bifurcation stenting, corresponding analytical tools for bifurcation analysis have been developed with extensive reporting schemes. Although intravascular ultrasound (IVUS) has been around for a long time as well, more recent radiofrequency analysis provides additional information about the vessel wall composition; likewise optical coherence tomography (OCT) provides detailed information about the positions of the stent struts and the quality of the stent placement. Combining the information from the X-ray lumenogram and the intravascular imaging devices is mentally a challenging task for the interventionalist. To support the registration of these intravascular images with the X-ray images, 3D QCA has been developed and registered with the IVUS or OCT images, so that at every position along the vessel of interest the luminal data and the vessel wall data by IVUS or the stent strut data by OCT can be combined. From the 3D QCA the selection of the optimal angiographic views can also be facilitated. It is the intention of this overview paper to provide an extensive description of the techniques that we have developed and validated over the past 30 years.

Key Words: Coronary artery disease; QCA; IVUS; OCT; 3D reconstruction; registration



Submitted Sep 16, 2011. Accepted for publication Sep 24, 2011.

DOI: 10.3978/j.issn.2223-3652.2011.09.03

Scan to your mobile device or view this article at: <http://www.thecdt.org/article/view/39>

Introduction

Quantitative Coronary Arteriography or QCA has come a long way, from the early 1980's with the angiograms being acquired on 35 mm cinefilm and requiring very expensive cinefilm projectors with optimal zooming for the quantitative analysis (1), to modern complete digital imaging with the images acquired at resolutions of 512^2 or 1024^2 pixels, and with the image data widely available throughout the hospital by means of Cardiovascular Picture Archiving and Communication Systems or CPACS systems. Major differences were of course that on cinefilm the coronary arteries were displayed as bright arteries on a darker background, and there was always an associated pincushion distortion caused by the concave input screen of the image intensifier. With the digital systems the arteries

are now displayed as dark vessels on a bright background and the modern flat-panel X-ray detectors are free from geometric distortions. Although there have been many years of debate about the resolution of cinefilm versus digital, the higher contrast resolution of the digital approach has compensated much of the higher spatial resolution of the 35 mm cinefilm, and thus digital has been completely accepted. Also, extensive validation studies have not proven major differences in accuracy and precision between cinefilm and digital: the variability in the analysis is on the order of about $\frac{1}{2}$ pixel, or 0.11 mm (2,3).

For many years, quantitative coronary arteriography (QCA) has been used in clinical research in the hospitals and in core laboratories to assess regression and progression of coronary obstructions in pharmacological interventions, and

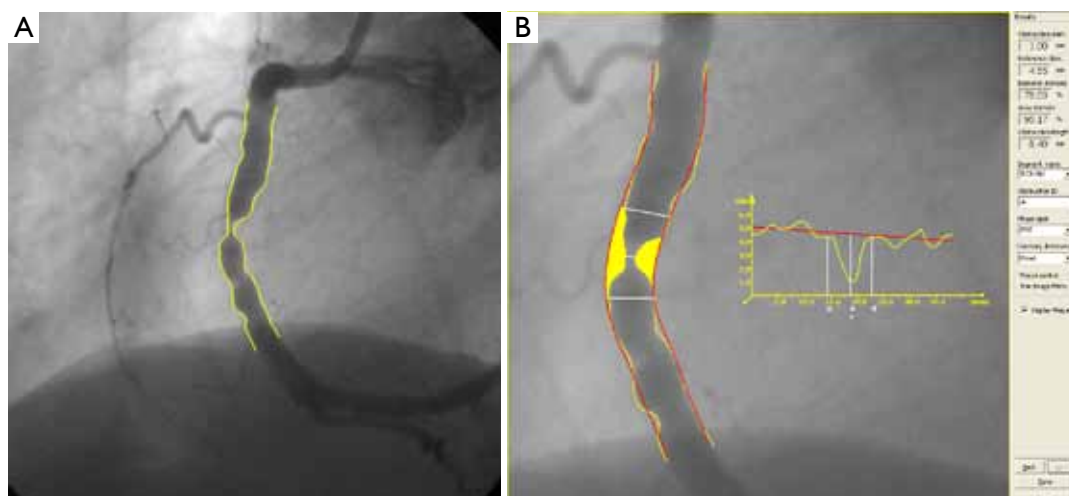


Figure 1 Example of a QCA straight analysis of a right coronary artery (RCA) mid segment. A. The arterial contours; B. The analysis results

of course for vessel sizing and the assessment of the efficacy of coronary interventions after the introduction of PTCA, bare-metal stents (BMS), drug-eluting stents (DES) and now also biodegradable stents. In all these cases, the analyses were done on straight vessels. However, since a number of years, bifurcation stenting has become of great interest, and in association with the European Bifurcation Club (EBC), the QCA software has been extended to allow also the quantitative analysis of the bifurcating morphology (4). This has proven to be a lot more difficult, in particular in defining what the normal sizes of the vessels adjacent to the bifurcation should be, given the complexity of the anatomy and different disease patterns. Validated solutions have been created and are now being used in clinical trials (5-10).

3D QCA has been around for quite some time from a few vendors, but it has never been applied on a wide scale in on-line situations for a number of reasons: segmentation not robust enough, too many user-interactions required and no clinical need. However, with the increasing applications of bifurcation stenting, there may be new opportunities, in combination with improved segmentation and reconstruction approaches. In particular, proper sizing of the length of the interventional devices has a significant effect on the long-term effect of the intervention (11), optimal viewing angles are more important in bifurcation stenting, and last but not least, latest developments also allow for the registration with intravascular devices, such as IVUS and OCT. This registration links the abnormalities as seen in the IVUS or OCT pullback sequences with the positions in either the 2D X-ray angiogram, or the 3D reconstruction. This software solution, which is now very robust and can be

used on-line, provides accurate information, such that the interventionalist does not need to rely on his/her mental registration capabilities alone anymore (12). It has been well recognized for many years that despite the wide availability of the angiogram and the QCA, an angiogram is only a lumenogram, and that the disease is in the vessel wall. For proper decision making purposes, the interventionalist must know what the composition is of the plaque. This was made possible with intravascular ultrasound, but with the advent of Virtual Histology and the iMAP, more information has become available, which has revived the field of intravascular ultrasound (13-17). Likewise, optical coherence tomography is now playing a major role in interventional cardiology (18-22).

In this review paper a brief overview will be given of the standard straight vessel analysis, followed by the more complex bifurcation analysis and finally by the latest developments in 3D QCA and the registration with IVUS or OCT. In each section references are given to validation studies. Most of the work presented is based on the Medis its analytical software packages (such as QAngio XA).

Straight vessel analysis

The procedure for a standard straight vessel segment is straight-forward, although obtaining robust arterial contours that require minimal manual editing requires mature and extensively validated software. An example of a straight QAngio XA analysis is given in *Figure 1* for a segment of a right coronary artery (RCA). After the manual definition of the start and endpoint of the segment, a

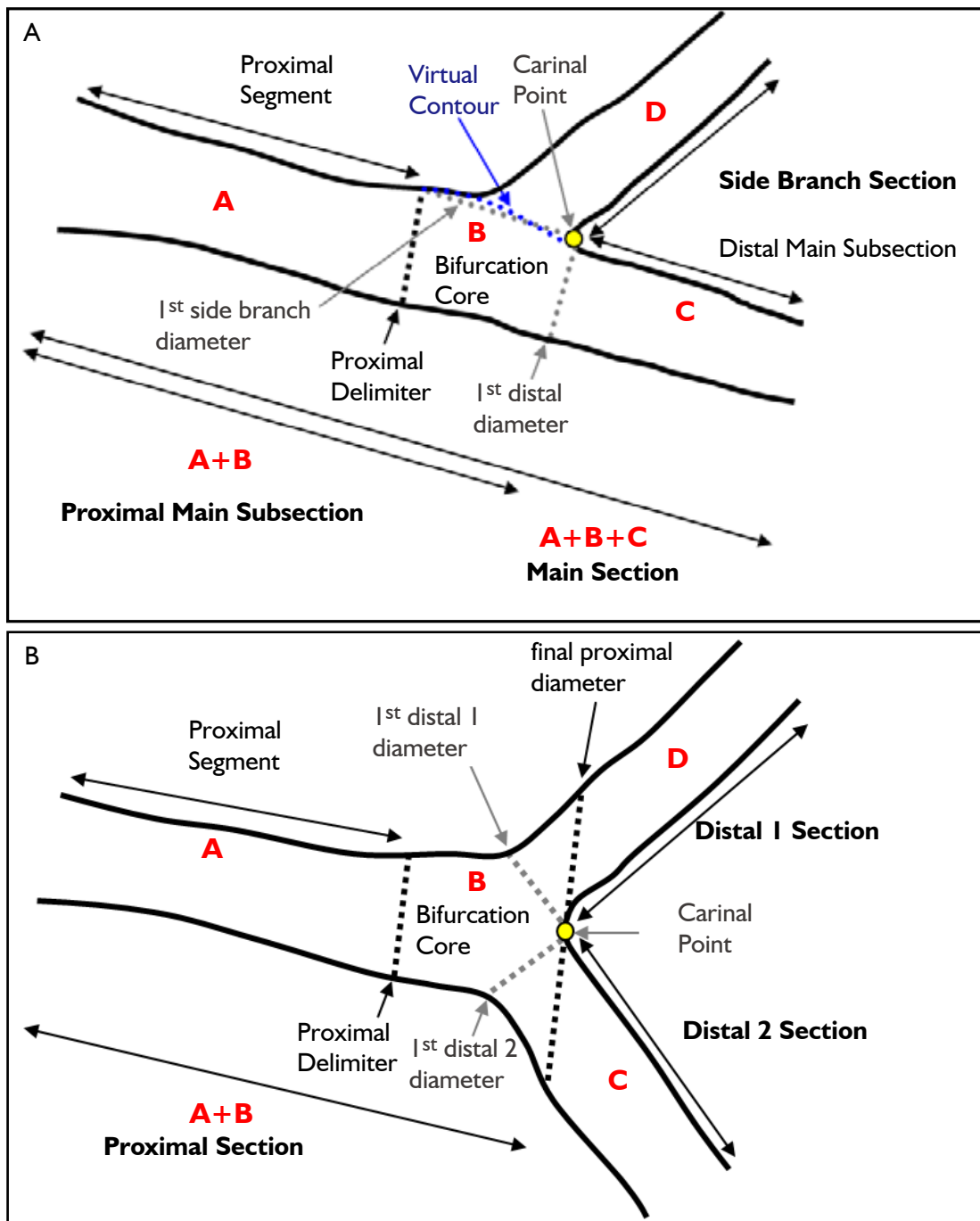


Figure 2 Schemes of the T-shape model and Y-shape model explaining the segments, proximal delimiter, interpolated contour and sections terminology. For each model, four segments that represent the building blocks of the models are generated by the software. A. In the T-shape model the bifurcation core is delineated by the proximal delimiter in the proximal main subsection and the carinal point (yellow point), which is flanked at one side by the first diameter of the distal main subsection, and at the other side by the interpolated contour between the proximal segment and the distal main subsection. Using this model, the arterial and reference diameters of the ostium of the side branch and the whole main section (including the transition within the carinal segment) can be accurately determined; B. In the Y-shape model the bifurcation core is delineated by the proximal delimiter in the proximal section and the carinal point (yellow point). Using this model, the arterial and reference diameters up to the carinal point and in the distal 1 and 2 segments can be determined accurately

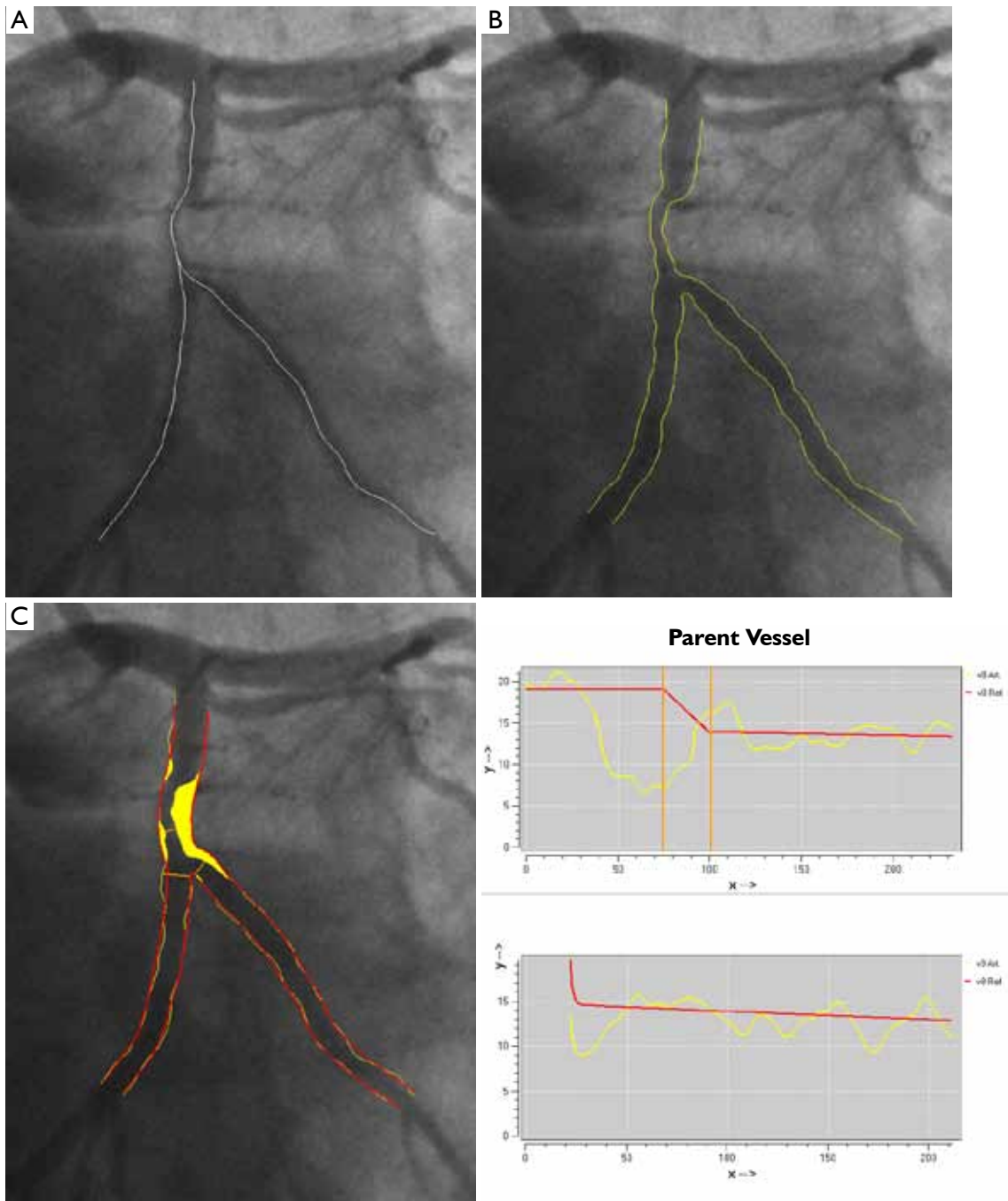


Figure 3 An example of the T-shape model of the bifurcation analysis. A. The two detected bifurcation pathlines, which are overlapping in the proximal segment; B. The detected arterial contours; C. The final analysis contours, plaque filling and the two corresponding diameter functions of the Main (a.k.a. Parent Vessel) and the Side Branch sections

pathline is detected automatically through the segment of interest. Next, the contour detection is carried out iteratively using the so-called minimal cost (MCA) contour detection algorithm in which all the grey level values along the vessel

of interest are taken into account. Of course, manual editing is possible if needed, but such interaction is again followed by a MCA iteration (*Figure 1A*). From the left and right arterial (yellow) lumen contours the size of the

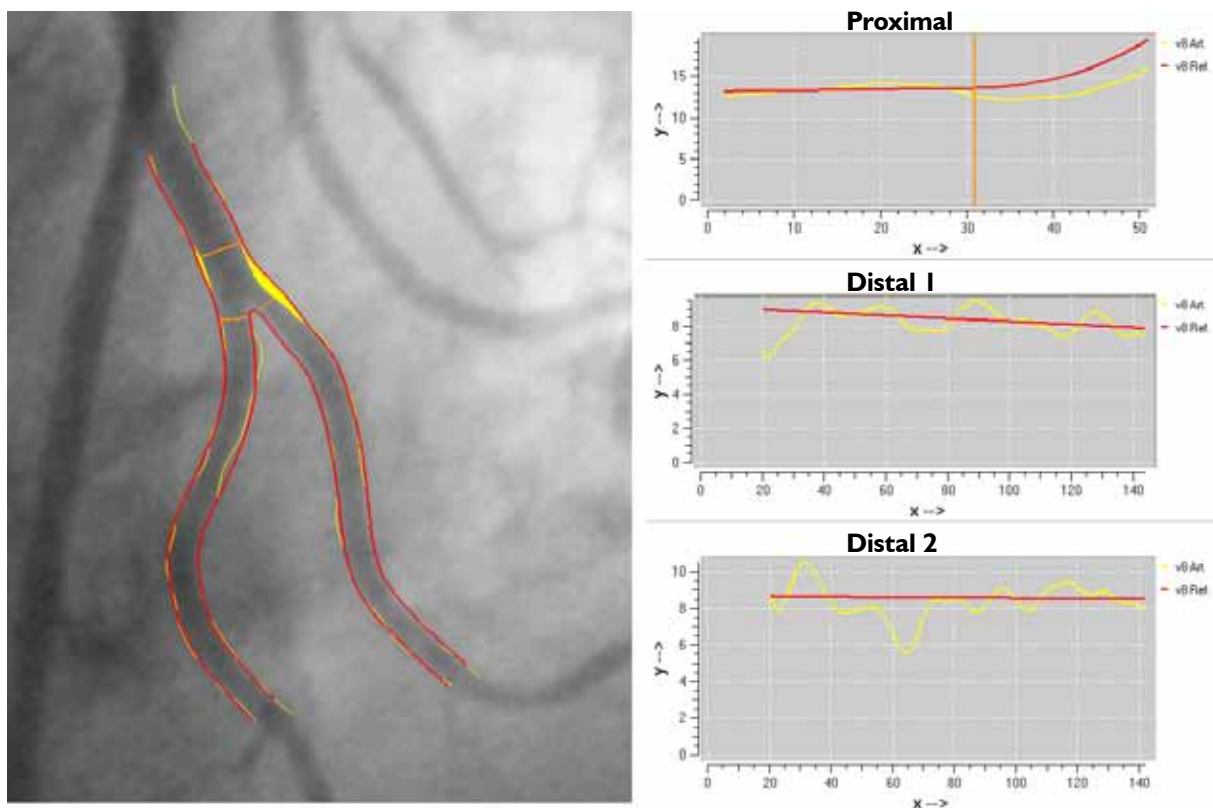


Figure 4 An example of the Y-shape model of the bifurcation analysis. The final analysis contours, plaque filling and the three corresponding diameter functions of the Proximal, Distal 1 and Distal 2 sections, respectively

vessel is calculated from start to end at intervals of about 0.1 mm and displayed in the arterial diameter function (yellow graph). From these numbers the interpolated-reference diameter function (red graph line) is derived, representing the situation of a healthy, non-diseased vessel segment. From this reference diameter function and the actual arterial contours, the reference contours (in red) can be reconstructed and positioned in the image along the vessel segment. The yellow area represents the plaque in the vessel in this particular angiographic view. From the calculated diameter functions, many parameters are derived automatically, including the site of the maximum percentage diameter stenosis, the obstruction diameter, the corresponding automatically determined reference diameter, and the extent of the obstruction. Additionally, other derived parameters include obstruction symmetry, inflow and outflow angles, the area of the atherosclerotic plaque, and functional information, such as the stenotic flow reserve or SFR. In the example of *Figure 1B*, the obstruction diameter is 1.00 mm and the reference diameter at the narrowing 4.55 mm, yielding a percentage

diameter stenosis of 78 %. The QAngio XA analytical software has been validated extensively by phantom studies, short-, medium- and long-term variability studies, inter- and intra-observer variability studies, inter-core-lab studies, etc (3).

Obtaining absolute numbers about the vessel sizes is not possible without carrying out a calibration procedure, which is usually performed on a non-tapering portion of a contrast-filled catheter using the MCA edge-detection procedure similar to that applied to the arterial segment. In this case, however, additional information is used in the edge-detection process because this part of the catheter is known to be characterized by parallel boundaries. It should also be recognized that the catheter calibration procedure is the weakest link in the analysis chain because of the variable image quality of the displayed catheters, and therefore deserves extra attention. Any error that is made in the calibration procedure has a direct effect on the calculated absolute vessel sizes. If one is only interested in relative values like the percentage diameter stenosis, the calibration procedure can be skipped.

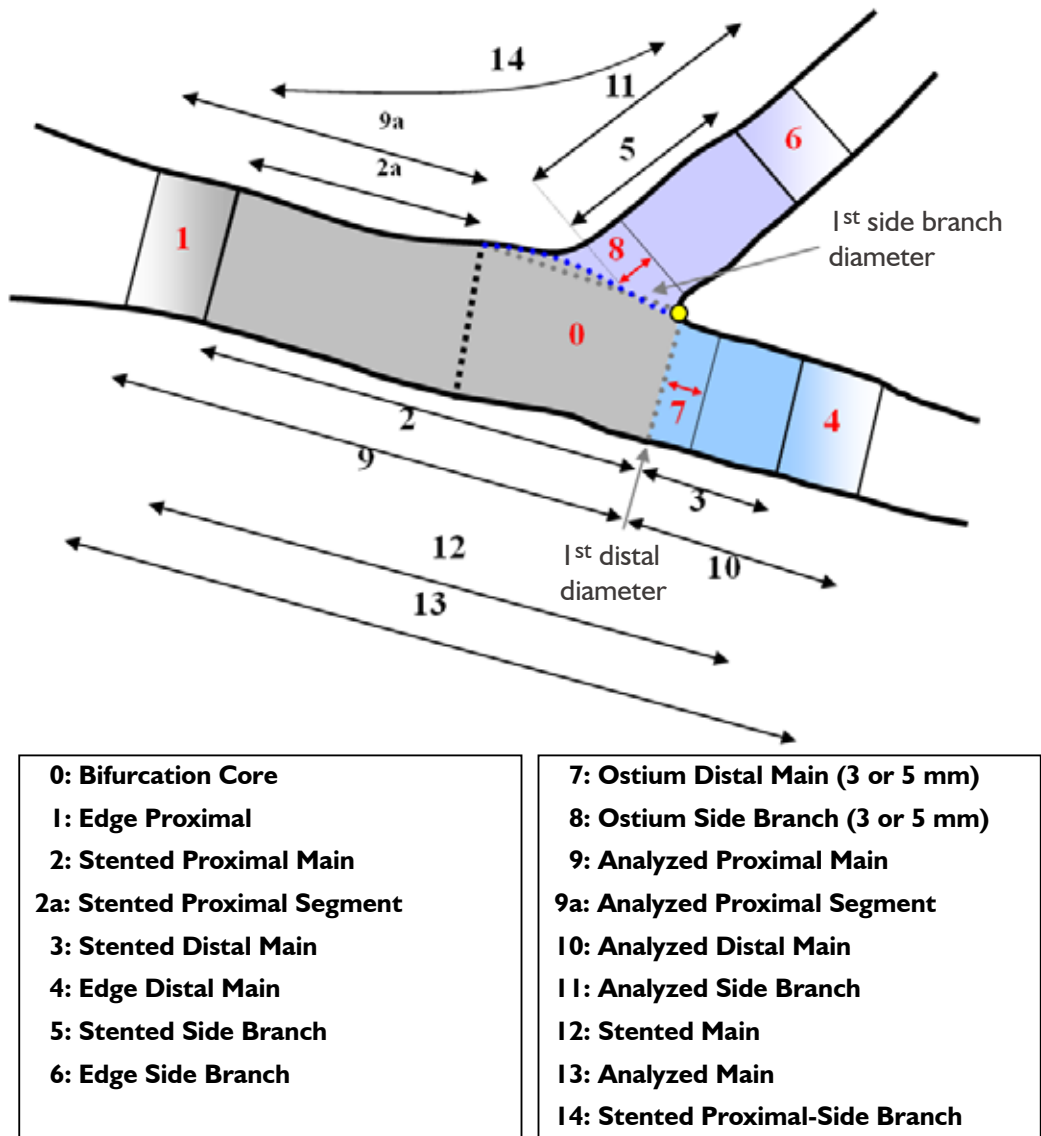


Figure 5 A schematic overview of the (sub) segments of the bifurcation analysis with edge segments

Bifurcation analysis

With the expanding practice of stenting coronary bifurcation lesions worldwide (23), the need for reliable, standardized and reproducible quantitative bifurcation analyses became apparent. There are two solutions available on the market, the CAAS Bifurcation software (Pie Medical, Maastricht, the Netherlands) and the QAngio XA version 7.2 bifurcation application (Medis medical imaging systems, Leiden, the Netherlands), which contains two bifurcation models: a T-shaped bifurcation model (suitable

for bifurcations with a standard side branch structure: *Figure 2A*) and Y-shaped bifurcation model (suitable for bifurcations with distal branches of equal size: *Figure 2B*). The particular advantage of these models is that they combine the proximal and two distal vessel segments with the bifurcation core, resulting in a total of two or three sections (depending on the model type), all derived from one analysis procedure, such that each of these sections has its own diameter function and associated parameter data.

The basic principles of the coronary bifurcation analyses of the two models can be summarized as follows. As a first

step, the user places three pathline points in the image to define the arterial bifurcation segment: a start point in the proximal segment and one end point in each of the two distal segments are required. Subsequently, independent of the model type, two pathlines are detected (*Figure 3A*) followed by the automated detection of the arterial contours of all three vessel segments using the MCA technique (*Figure 3B*).

The bifurcation core of the T-shape model is defined as the area between the automatically determined proximal delimiter in the proximal main subsection (the position of which is independent of the presence of a lesion) and the carinal point, which is flanked at one side by the first diameter of the distal main subsection and at the other side by the interpolated contour between the proximal segment and distal main subsection (*Figure 2A*). From the arterial contours and the interpolated contour, two sections are defined: the main section (i.e. the proximal segment, distal main subsection and bifurcation core segment merged) and the side branch section (*Figure 2A*). For the main section the arterial diameter function is calculated following the conventional straight analysis approach, while for the side branch section the ostial analysis approach is followed (3,5), making sure that the arterial diameters at the ostium of the side branch are measured properly.

Due to the “step down” phenomenon, it is not a trivial task to derive a suitable reference diameter function for the entire main section. Therefore, the calculation of the reference diameter function is based on each of the three segments separately. By this approach, it is assured that for both the proximal segment and distal main subsection the (interpolated) reference diameter functions are only based on the arterial diameters outside the bifurcation core. Finally, the reference diameter function of the bifurcation core is based on the reconstruction of a smooth transition between the proximal and distal vessel diameters. As a result, the reference diameter function graph of the entire main section will be displayed as one function, which is composed of three different straight reference lines that are linked together. For the side branch section an “ostial” reference diameter function calculation is used (3,5), which is displayed as one function, which is straight and slightly curved proximally (*Figure 3C*).

The bifurcation core of the Y-shape model is defined as the area between the automatically determined proximal delimiter in the proximal section and the carinal point (*Figure 2B*). From the arterial contours and by using the carinal point, three sections are defined: the proximal section (i.e. the proximal and bifurcation core segments merged), the distal 1 section and the distal 2 section (*Figure 2B*). For each of these sections

the corresponding arterial diameter functions are calculated following the conventional straight analysis approach (3,5). This method guarantees that within the bifurcation core the arterial diameters are measured in their fullest extent (e.g., important for skirt stenting).

In order to derive a suitable reference diameter function for each section, again the calculation of the reference diameter function is based on each of the segments separately. The reference diameter function of the bifurcation core itself is based on reconstructed reference contours between the proximal and two distal segments. As a result, the reference diameter function graph of the entire proximal section will be displayed as one function, which is straight for the proximal segment and curved in the bifurcation core. The two reference diameter functions of the distal sections will each be displayed as one function and are straight (*Figure 4*).

The reported bifurcation analysis results of all sections (both models) will be a complete listing of the angiographic parameters similar to the conventional straight QCA, including the obstruction, reference, minimum, maximum, mean diameters and areas, the percent diameter and area stenosis, as well as the vessel and lesion lengths.

Additionally, an option for bifurcation with edge segment analysis will be available for the assessment of (drug eluting) stent segments and the corresponding stent- and ostial edge segments (*Figure 5*). For each of these (sub)segments the complete parameter set including some edge specific parameters (e.g., MLD position relative to the stent start or segment start position, etc.) will be reported, to allow to study the regression and progression of the bifurcation lesion to the fullest.

The QAngio XA Bifurcation analysis software V7.2 has been validated extensively by phantom studies, clinical studies and observer variability studies (5,6).

3D QCA and registration with IVUS and OCT

Over the past decades, the continuous developments in coronary visualization and quantitative systems have been motivated by the increasing need to better understand and assess coronary atherosclerosis and by the on-line need for support of coronary interventions in cardiac catheterization laboratories. Recently developed three-dimensional quantitative coronary angiography (3D QCA) systems aimed to resolve some of the limitations in conventional two-dimensional (2D) analysis (1,3,4) and hence, to extend its capacity and reliability in assessing the true cross-sectional area and length dimensions of coronary vascular

structures. It has been demonstrated that 3D QCA can accurately assess vessel segment length and diameter(24-26), as well as the optimal viewing angles (11,27-29) for the subsequent interventional stent-procedure. By using 3D QCA and based on such more accurate 3D data, clinical decision making can be affected, thus possibly leading to a more efficient and economic usage of stents in percutaneous coronary intervention (PCI) (30). This may have significant impact in today's cost-constrained health care systems.

Despite the fact that the 3D angiographic reconstruction has important potential values, the foremost limitation of X-ray angiography-based systems remains the inability to image beyond the vessel lumen as only the contrast lumen is visualized. In other words, the 3D reconstructed vessel remains a lumenogram, though with better 3D capabilities. Thus, early stages of plaque formation may not be evident with X-ray angiography due to the occurrence of coronary artery remodeling (31), and vulnerable plaques can not be recognized for possible implementations of measures to prevent these from rupturing. These limitations have been well addressed by intravascular tomography-based imaging techniques, among which grey scale intravascular ultrasound (IVUS) is a well-established and validated modality. IVUS provides a wealth of information including vessel wall composition, which is crucial to the assessment of coronary atherosclerosis. Later on, the role of intravascular tomography-based imaging techniques was greatly enhanced by the radio-frequency IVUS data analysis for plaque characterization (e.g., Virtual Histology and iMAP) and by optical coherence tomography (OCT) for the assessment of the thin fibrous cap atheromas and malapposition of stent struts, respectively. These new imaging techniques have greatly extended the capabilities in the assessment of coronary artery disease. However, the fact that intravascular tomography-based images do not preserve the global topology information could lead to erroneous interpretations. Although a longitudinal view (L-View) is available in most IVUS/OCT consoles to provide an overview of the pullback series, the presentation of the L-View by stacking cross-sectional images along a straightened version of the catheter pullback trajectory is a very unnatural way of conceptualization. As a result, the interpretation can be quite challenging.

Given the different but complementary perspectives provided by X-ray angiography (XA) and IVUS/OCT, the fusion/integration of the two imaging modalities by using XA as a roadmap while exploiting detailed vessel wall information from IVUS/OCT will benefit the

interpretation of coronary artery disease and the guidance of coronary interventions. In current routine clinical practice, the interventionalist must mentally establish the correspondence between the XA and IVUS/OCT images. This process is not always easy, especially when lumen narrowing is not clearly evident by the X-ray images or when the lesion is long diffused, and no side branch is present in the neighborhood of the lesion borders. Thus, XA-IVUS/OCT integrated systems are currently requested in the market to better support coronary interventions. The clinical applicability of such fused/integrated systems depends to a great extent on the reliability and robustness of the co-registration step. Once a reliable correspondence between angiographic and IVUS/OCT images is established, the issue of fusing/integrating information from the two image modalities becomes relevant.

In the following paragraphs our approach for the 3D reconstruction and co-registration with IVUS/OCT is described and the results of both phantom and in-vivo validations are presented.

Three-dimensional angiographic reconstruction

Accurate and robust 3D angiographic reconstruction is the foremost important step in the XA-IVUS/OCT co-registration. Early research on 3D reconstruction can be traced back to decades ago (32,33). However, clinic-ready systems were announced only in recent years and there has not been a widespread acceptance of such systems in routine clinical practice. One of the reasons is due to the fact that mechanical distortions in X-ray systems and noisy angiographic images in routine clinical acquisitions could significantly affect the reliability and robustness of the 3D reconstruction and analysis. For monoplane X-ray angiographic acquisitions, the shift of the whole coronary tree due to the patient's respiration or the non-isocentric condition could greatly deteriorate the system's reliability. Such system distortions should be corrected before or during the 3D angiographic reconstruction.

To come up with a practical and attractive workflow, we have developed a new approach by using only one to three pairs of reference points for the correction of system distortions. In case of the presence of small perspective projection angles for noisy angiographic images, the reliability and robustness of the angiographic reconstruction are further improved by building a distance transformation matrix and by searching for the optimal corresponding path in the matrix for the refinement of correspondence

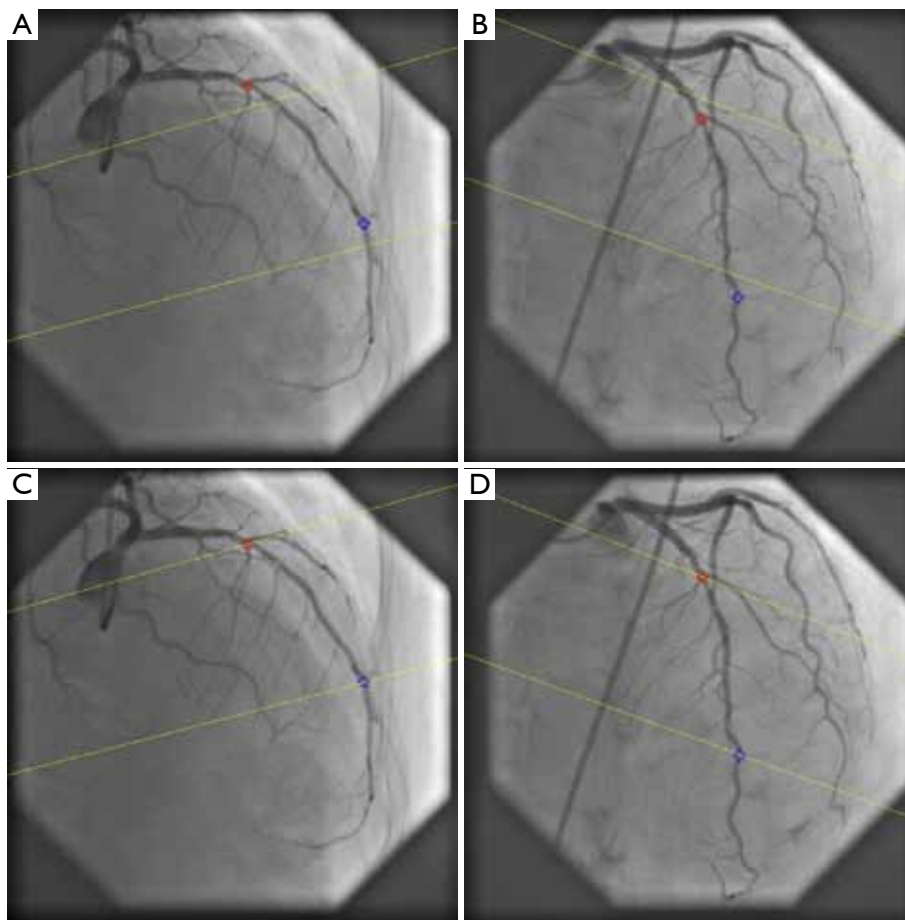


Figure 6 Automated correction of system distortions in the image geometry for the 3D angiographic reconstruction. A and B are the two angiographic views (31 RAO, 33 Cranial and 31 LAO, 30 Cranial) selected for the 3D reconstruction. Before the correction, the two epipolar lines did not go through their corresponding reference points, being the red and blue landmarks; C and D show the results after the automated correction of the system distortion. The two epipolar lines now go right through their corresponding reference points in both projection views

between the two angiographic views (11). The approach has been validated with high accuracy in both phantom and in-vivo studies (11,24,26). In short, the 3D angiographic reconstruction consists of only a few major steps: (i) two image sequences acquired at two arbitrary angiographic views with projection angles at least 25 degrees apart are loaded; (ii) properly contrast-filled end-diastolic (ED) frames of these angiographic image sequences are selected; (iii) one to three anatomical markers, e.g., bifurcations, are identified as reference points in the two angiographic views for the automated correction of angiographic system distortions (11); (iv) the vessel segment of interest is defined and automated 2D lumen edge detection is performed using our extensively validated QCA algorithms (1,2,6,34); (v)

automated 3D reconstruction and modeling techniques are performed.

An example of step three, correction the system distortions in the image geometry for the 3D angiographic reconstruction, is given in *Figure 6A and 6B*. The two bifurcation points (carina) in the left anterior descending artery (LAD) were identified as reference points and their epipolar lines, being the projection of the X-ray beam directed towards a particular point on one of the projections onto the second projection, were presented in the two angiographic views (31 RAO, 33 Cranial and 31 LAO, 30 Cranial, respectively). Due to the system distortions, the epipolar lines did not go through their corresponding reference points. After applying the automated correction

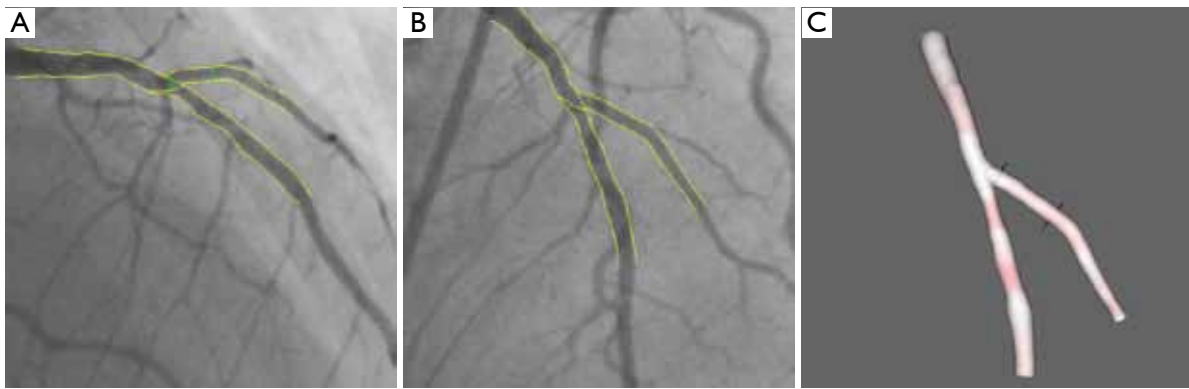


Figure 7 Three-dimensional coronary bifurcation reconstruction. A and B show the two angiographic views with lumen contours superimposed on the LAD/Diagonal bifurcation; C shows the 3D reconstructed bifurcation at optimal viewing angle (40 LAO, 56 Cranial)

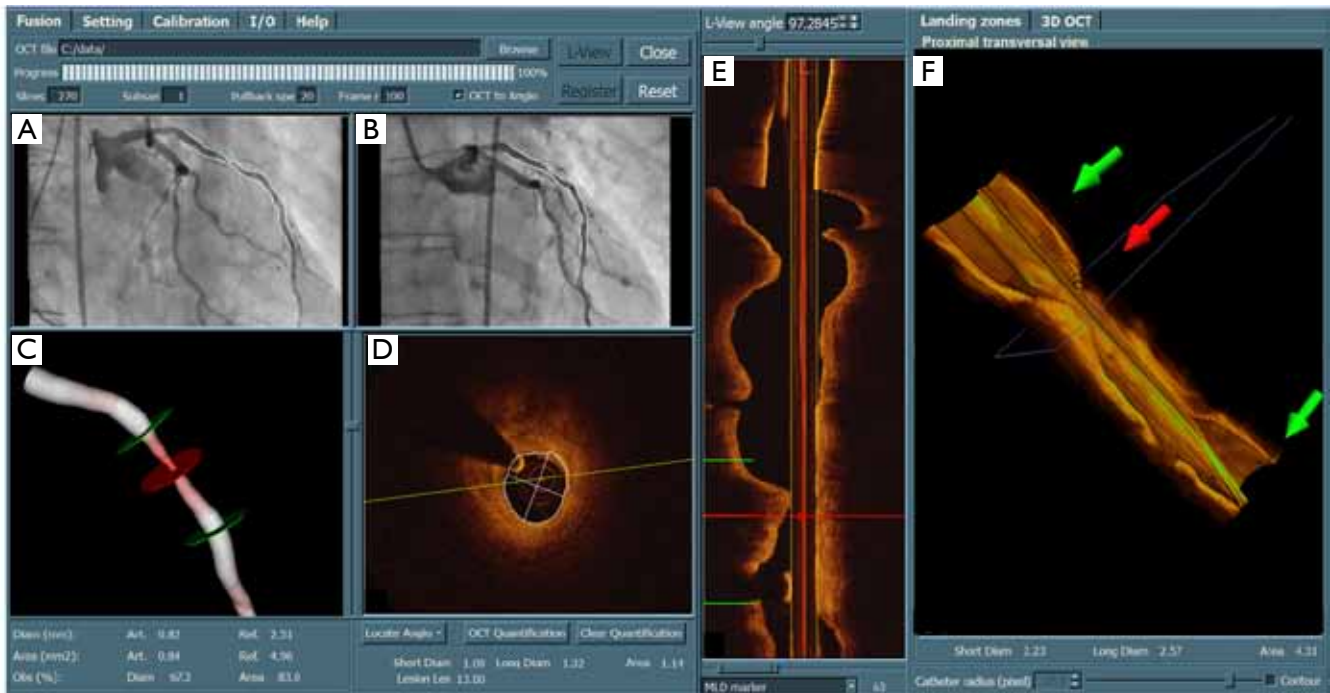


Figure 8 Three-dimensional quantitative coronary angiography (3D QCA) and its registration with 3D optical coherence tomography (OCT). A and B are the two angiographic views; C is the reconstructed vessel segment in color-coded fashion; D is the OCT cross-sectional view corresponding to the middle (red) marker; E is the OCT longitudinal view; and F is the 3D OCT image. After the registration, the corresponding markers in different views (A, B, C, D, and F) were synchronized, allowing the assessment of lumen dimensions from both imaging modalities at every corresponding position along the vessel segment

of the system distortion, as shown in *Figure 6C, D*, the epipolar lines now go right through their corresponding reference points in both angiographic views, demonstrating the success of this automated procedure.

When subsequently the steps four and five are applied, the 3D reconstructed straight vessel or bifurcation is

obtained. In *Figure 7A, B* the two angiographic views with lumen contours superimposed on the LAD/Diagonal bifurcation are shown. Finally, *Figure 7C* presents the reconstructed LAD/Diagonal bifurcation at its optimal viewing angle, being 40 LAO, 56 Cranial, by which the overlap between the LAD and the Diagonal at the ostium is

minimal. The proximal bifurcation angle, i.e., the take-off angle, and the distal bifurcation angle, i.e., the carina angle, are 139° and 44°, respectively.

XA-IVUS/OCT registration

Under the condition that the motorized transducer pullback with constant speed is used in the IVUS/OCT image acquisition, the rationale for the co-registration of XA images with IVUS/OCT pullback series is to use the spatial relationship between vessel segment (by means of lumen or centerline) and IVUS/OCT pullback trajectory. Conventional registration approaches (35-37) would require the reconstruction of the IVUS/OCT transducer path from two angiographic views acquired, and assume it to be the pullback trajectory so that the IVUS/OCT cross-sectional images can be aligned along the trajectory. This is not a trivial task due to the difficulty in segmenting both IVUS/OCT catheter and vessel lumen and the requirement of a second angiographic view for the IVUS/OCT catheter, which is not always included in the current workflow. The assumption of IVUS/OCT transducer path as pullback trajectory could also be jeopardized by the fact that spatial displacement of the catheter could occur inside the vessel after the pullback machine is switched on, in order to reach the state of minimum bending energy. It has been reported that there was significant delay from the moment the IVUS pullback machine was switched on and the moment the transducer tip really started to move (37).

In order to have a rapid and straightforward solution for the on-line XA-IVUS/OCT registration that could assist coronary interventions and would fit most into the current workflow in catheterization laboratories, we have taken a different approach by estimating the axial position of each IVUS/OCT cross-sectional image from the reconstructed vessel centerline, based on the curvature information and hence, to skip the reconstruction of the pullback trajectory (12). By this approach, the disadvantage of using diluted contrast agent during angiographic image acquisitions, as required by conventional registration approaches in order to simultaneously visualize the lumen and the imaging catheter, was resolved and as a result, the quality of 3D QCA was improved and less manual corrections were required in the lumen edge detection. The approach only requires the operator to reconstruct the vessel centerline from the angiographic images (which is a standard module in our 3D QCA software package) and register it with IVUS/OCT pullback series by indicating a

baseline position in the vessel centerline that corresponds to the same axial position in IVUS/OCT. Such baseline positions can be found in anatomical or mechanical landmarks visualized in both angiographic and IVUS/OCT images, e.g., side branches and stent borders. In case of blurred angiographic images, image enhancement techniques (38) can be used to increase the visibility of detailed image structures.

After the registration, the markers superimposed on the angiographic views and the IVUS/OCT L-View are now synchronized. The interpretation of vessel dimensions becomes more comprehensive and the interventionalist knows now exactly where in the XA images the stent should be positioned based on the IVUS/OCT data. An example of integrating angiographic and IVUS/OCT images after the registration is given by *Figure 8*. The stenting-position defined by the proximal and distal landing-zone markers has been mapped onto the two angiographic views in the top left panel (the two green markers that are superimposed on the angiographic views). In addition, the luminal contours were automatically detected in the OCT cross-sectional images by using a new minimum cost algorithm and the diameter and lumen area can be compared with the measurements from the 3D QCA. In this case, short diameter, long diameter, and lumen area at the position indicated by the middle (red) marker were 1.08 mm, 1.32 mm, and 1.14 mm² by OCT, as compared with 0.82 mm, 1.30 mm, and 0.84 mm² by 3D QCA, respectively.

Discussion

Drug-eluting stents have proven to be able to reduce in-stent restenosis after coronary interventions (39-41); however, the efficacy depends on the ability of the interventionalist to choose the optimal course of treatment and to implement the chosen course of action properly. Geographic mismatch due to suboptimal stent selection and positioning could significantly impact the short and long term outcome of the stent-procedure (42,43). Sophisticated imaging and quantification tools are therefore demanded to guide the interventionalist to assess the true vessel dimensions, lesion location and extension for the optimization of the stent-procedure.

Quantitative coronary angiography was first developed to quantify vessel motion and the effects of pharmacological agents on the regression and progression of coronary artery disease (44). It has developed substantially over the past decades and has been applied worldwide for

research and clinical purposes, in both off-line and on-line situations (3). Recently developed 3D systems based on routine angiographic projections have emerged as a new tool for the on-line guiding of coronary interventions. By resolving some of the well-known limitations in standard 2D analysis, e.g., vessel foreshortening and out-of-plane magnification (45), 3D QCA could provide more reliable assessments of lumen dimensions including length, diameter, and bifurcation angles (24,26). In addition, the 3D angiographic reconstruction enables the subsequent automated determination of optimal viewing angles (11,27), by which foreshortening and overlap are minimized and the visualization of the target vessel is improved.

Thanks to the capacity and high resolution in imaging individual cross-sections of the coronary artery, IVUS and OCT have greatly improved our understanding of coronary atherosclerosis and the tissue responses after stent implantation. The role of IVUS/OCT in assessing plaque extent and distribution for optimal treatment planning has been well acknowledged. However, the ability in implementing the planned course by angioplasty has been limited by the difficulty in establishing the correspondence between the IVUS/OCT images with the angiographic images. For example, to position the stent, the current workflow by mentally mapping the planned stenting-position from IVUS/OCT to XA fluoroscopy could be quite challenging when no landmark is available in the neighborhood of the stenting-position and accurate positioning is important to ensure complete lesion coverage and to prevent the undesirable responses to the stent expansion, e.g., stenting long diffused lesions with calcium deposited at the borders. In other cases where the diseased vessel has multiple side branches, like in the LAD with many septal and diagonal branches, the mental mapping could be confused or even become completely mismatched due to the fact that not all side branches are well presented in the L-View of IVUS/OCT. In such cases, the XA-IVUS/OCT co-registration could establish a point-to-point correspondence between angiographic and IVUS/OCT images. As a result, the deployment of the stent to the targeted position is simplified and more clearer.

Despite of its attractive clinical perspectives, an optimal integration of 3D XA and IVUS or OCT in the current setting of catheterization laboratories is currently not available. The data connectivity is a significant bottleneck for such an integration to be used in on-line mode. Demonstration projects have clearly indicated the clinical value of the registration of OCT and 3D QCA for

supporting coronary interventions, e.g., for verifying the wire position before dilating the stent at the bifurcation (46). Therefore, it is desirable that the XA, IVUS/OCT, as well as 3rd party imaging vendors will cooperate to make the integration clinically acceptable with a seamless workflow in the near future.

Conclusions

The new XA-IVUS/OCT registration approach is a straight-forward and reliable solution for the three-dimensional integration/combination of X-ray angiographic and IVUS/OCT imaging. It provides the interventionalist with detailed information about vessel size and plaque size at every position along the vessel of interest, making this a suitable tool during the actual intervention.

Acknowledgements

Disclosure: The authors declare no conflict of interest.

References

1. Reiber JH, Serruys PW, Kooijman CJ, et al. Assessment of short-, medium-, and long-term variations in arterial dimensions from computer-assisted quantitation of coronary cineangiograms. *Circulation* 1985;71:280-8.
2. Reiber JH, van der Zwet PM, Koning G, et al. Accuracy and precision of quantitative digital coronary arteriography: observer-, short-, and medium-term variabilities. *Cathet Cardiovasc Diagn* 1993;28:187-98.
3. Reiber JHC, Tuinenburg JC, Koning G, et al. Quantitative coronary arteriography. In: *Coronary Radiology 2nd Revised Edition*, Oudkerk M, Reiser MF (Eds.), Series: Medical Radiology, Sub series: Diagnostic Imaging, Baert AL, Knauth M, Sartor K (Eds.). Springer-Verlag, Berlin-Heidelberg 2009:41-65.
4. Lansky A, Tuinenburg J, Costa M, et al; European Bifurcation Angiographic Sub-Committee. Quantitative angiographic methods for bifurcation lesions: a consensus statement from the European Bifurcation Group. *Catheter Cardiovasc Interv* 2009;73:258-66.
5. Janssen JP, Rares A, Tuinenburg JC, et al. New approaches for the assessment of vessel sizes in quantitative (cardio-) vascular X-ray analysis. *Int J Cardiovasc Imaging* 2010;26:259-71.
6. Tuinenburg JC, Koning G, Rares A, et al. Dedicated bifurcation analysis: basic principles. *Int J Cardiovasc*

- Imaging 2011;27:167-74.
7. Collet C, Costa RA, Abizaid A. Dedicated bifurcation analysis: dedicated devices. *Int J Cardiovasc Imaging* 2011;27:181-8.
 8. Steigen TK, Maeng M, Wiseth R, et al. Nordic PCI Study Group. Randomized study on simple versus complex stenting of coronary artery bifurcation lesions: The Nordic bifurcation study. *Circulation* 2006;114:1955-61.
 9. Holm NR, Højdaahl H, Lassen JF, et al. Quantitative coronary analysis in the Nordic Bifurcation studies. *Int J Cardiovasc Imaging* 2011;27:175-80.
 10. Ng VG, Lansky AJ. Novel QCA methodologies and angiographic scores. *Int J Cardiovasc Imaging*. 2011;27:157-65.
 11. Tu S, Koning G, Jukema W, et al. Assessment of obstruction length and optimal viewing angle from biplane X-ray angiograms. *Int J Cardiovasc Imaging* 2010;26:5-17.
 12. Tu S, Holm NR, Koning G, et al. Fusion of 3D QCA and IVUS/OCT. *Int J Cardiovasc Imaging* 2011;27:197-207.
 13. Costa RA, Costa MA, Moussa ID. Bifurcation lesion morphology and intravascular ultrasound assessment. *Int J Cardiovasc Imaging* 2011;27:189-96.
 14. Huisman J, Hartmann M, von Birgelen C. Ultrasound and light: friend or foe? On the role of intravascular ultrasound in the era of optical coherence tomography. *Int J Cardiovasc Imaging* 2011;27:209-14.
 15. García-García HM, Gogas BD, Serruys PW, et al. IVUS-based imaging modalities for tissue characterization: similarities and differences. *Int J Cardiovasc Imaging* 2011;27:215-24.
 16. Gogas BD, Farooq V, Serruys PW, et al. Assessment of coronary atherosclerosis by IVUS and IVUS-based imaging modalities: progression and regression studies, tissue composition and beyond. *Int J Cardiovasc Imaging* 2011;27:225-37.
 17. Brugaletta S, Costa JR Jr, Garcia-Garcia HM. Assessment of drug-eluting stents and bioresorbable stents by grayscale IVUS and IVUS-based imaging modalities. *Int J Cardiovasc Imaging* 2011;27:239-48.
 18. Prati F, Jenkins MW, Di Giorgio A, et al. Intracoronary optical coherence tomography, basic theory and image acquisition techniques. *Int J Cardiovasc Imaging* 2011;27:251-8.
 19. Mehanna EA, Attizzani GF, Kyono H, et al. Assessment of coronary stent by optical coherence tomography, methodology and definitions. *Int J Cardiovasc Imaging* 2011;27:259-69.
 20. Tahara S, Chamié D, Baibars M, et al. Optical coherence tomography endpoints in stent clinical investigations: strut coverage. *Int J Cardiovasc Imaging* 2011;27:271-87.
 21. Kubo T, Xu C, Wang Z, et al. Plaque and thrombus evaluation by optical coherence tomography. *Int J Cardiovasc Imaging* 2011;27:289-98.
 22. Stefano GT, Bezerra HG, Attizzani G, et al. Utilization of frequency domain optical coherence tomography and fractional flow reserve to assess intermediate coronary artery stenoses: conciliating anatomic and physiologic information. *Int J Cardiovasc Imaging* 2011;27:299-308.
 23. Lefèvre T, Louvard Y, Morice MC, et al. Stenting of bifurcation lesions: a rational approach. *J Interv Cardiol* 2001;14:573-85.
 24. Tu S, Holm NR, Koning G, et al. The impact of acquisition angle differences on three-dimensional quantitative coronary angiography. *Catheter Cardiovasc Interv* 2011;78:214-22.
 25. Rittger H, Schertel B, Schmidt M, et al. Three-dimensional reconstruction allows accurate quantification and length measurements of coronary artery stenoses. *EuroIntervention* 2009;5:127-32.
 26. Tu S, Huang Z, Koning G, et al. A novel three-dimensional quantitative coronary angiography system: In-vivo comparison with intravascular ultrasound for assessing arterial segment length. *Catheter Cardiovasc Interv* 2010;76:291-8.
 27. Tu S, Hao P, Koning G, et al. In vivo assessment of optimal viewing angles from X-ray coronary angiography. *EuroIntervention* 2011;7:112-20.
 28. Green NE, Chen SY, Hansgen AR, et al. Angiographic views used for percutaneous coronary interventions: a three-dimensional analysis of physician-determined vs. computer-generated views. *Catheter Cardiovasc Interv* 2005;64:451-9.
 29. Sadamatsu K, Sagara S, Yamawaki T, et al. Three-dimensional coronary imaging for the ostium of the left anterior descending artery. *Int J Cardiovasc Imaging* 2009;25:223-8.
 30. Gollapudi RR, Valencia R, Lee SS, et al. Utility of three-dimensional reconstruction of coronary angiography to guide percutaneous coronary intervention. *Catheter Cardiovasc Interv* 2007;69:479-82.
 31. Glagov S, Weisenberg E, Zarins CK, et al. Compensatory enlargement of human atherosclerotic coronary arteries. *N Engl J Med* 1987;316:1371-5.
 32. Dumay ACM. Image reconstruction from biplane angiographic projections. Dissertation 1992, Delft University of Technology, the Netherlands.

33. Wahle A, Wellnhofer E, Mugaragu I, et al. Assessment of diffuse coronary artery disease by quantitative analysis of coronary morphology based upon 3-D reconstruction from biplane angiograms. *IEEE Trans Med Imaging* 1995;14:230-41.
34. Janssen JP, Koning G, de Koning PJ, et al. A new approach to contour detection in x-ray arteriograms: the wavecontour. *Invest Radiol* 2005;40:514-20.
35. Slager CJ, Wentzel JJ, Schuurbiens JC, et al. True 3-dimensional reconstruction of coronary arteries in patients by fusion of angiography and IVUS (ANGUS) and its quantitative validation *Circulation* 2000;102:511-6.
36. Wahle A, Lopez JJ, Olszewski ME, et al. Plaque development, vessel curvature, and wall shear stress in coronary arteries assessed by X-ray angiography and intravascular ultrasound. *Med Image Anal* 2006;10:615-31.
37. Rotger D, Radeva P, Canero C, et al. Corresponding IVUS and angiogram image data. *Proc Comput Cardiol* 2001;28:273-6.
38. Tu S, Koning G, Tuinenburg JC, et al. Coronary angiography enhancement for visualization. *Int J Cardiovasc Imaging* 2009;25:657-67.
39. Moses JW, Leon MB, Popma JJ, et al. Sirolimus-eluting stents versus standard stents in patients with stenosis in a native coronary artery. *N Engl J Med* 2003;349:1315-23.
40. Stone GW, Ellis SG, Cox DA, et al. A polymer-based, paclitaxel-eluting stent in patients with coronary artery disease. *N Engl J Med* 2004;350:221-31.
41. Stone GW, Moses JW, Ellis SG, et al. Safety and efficacy of sirolimus- and paclitaxel-eluting coronary stents. *N Engl J Med* 2007;356:998-1008.
42. Fujii K, Carlier SG, Mintz GS, et al. Stent underexpansion and residual reference segment stenosis are related to stent thrombosis after sirolimus-eluting stent implantation: an intravascular ultrasound study. *J Am Coll Cardiol* 2005;45:995-8.
43. Costa MA, Angiolillo DJ, Tannenbaum M, et al. Impact of stent deployment procedural factors on long-term effectiveness and safety of sirolimus-eluting stents (final results of the multicenter prospective STLLR trial). *Am J Cardiol* 2008;101:1704-11.
44. Brown BG, Bolson E, Frimer M, et al. Quantitative coronary arteriography: estimation of dimensions, hemodynamic resistance, and atheroma mass of coronary artery lesions using the arteriogram and digital computation. *Circulation* 1977;55:329-37.
45. Koning G, Hekking E, Kemppainen JS, et al. Suitability of the Cordis Stabilizer marker guide wire for quantitative coronary angiography calibration: an in vitro and in vivo study. *Catheter Cardiovasc Interv* 2001;52:334-41.
46. Holm NR, Tu S, Christiansen EH, et al. Use of three-dimensional optical coherence tomography to verify correct wire position in a jailed side branch after main vessel stent implantation. *EuroIntervention* 2011;7:528-9.

Cite this article as: Reiber JH, Tu S, Tuinenburg JC, Koning G, Janssen JP, Dijkstra J. QCA, IVUS and OCT in interventional cardiology in 2011. *Cardiovasc Diagn Ther* 2011;1:57-70. DOI: 10.3978/j.issn.2223-3652.2011.09.03